Mobile Networks and Applications
https://doi.org/10.1007/s11036-018-1036-9

Doppler Effect in the Acoustic Ultra Low Frequency Band for Wireless Underwater Networks

A.-M. Ahmad[1] · J. Kassem[1] · M. Barbeau[2] · E. Kranakis[2] · S. Porretta[2] · J. Garcia-Alfaro[3]

© Springer Science+Business Media, LLC, part of Springer Nature 2018

Abstract
It is well known that communication is affected by the change in frequency of a signal for an observer that is moving relative to the source. As a result of the motion of either the source or the observer, successive waves are emitted from a position that may get closer or further to the observer. This phenomenon, known as Doppler effect, also affects underwater acoustic waves used for communications between Autonomous Underwater Vehicles (AUVs), Underwater Sensors (USs) and remote operators. There have been few studies on the impact of Doppler shift in underwater communications. Assuming underwater communications using acoustic waves, in this paper we study the Doppler effect in relation to the half-power bandwidth and distance in the Ultra Low Frequency (ULF) band (i.e., from 0.3 to 3 kHz). We investigate two specific issues. Firstly, the maximum shift that can be expected on underwater links in the ULF band. Secondly, the maximum frequency drift, and associated patterns, that can happen during the reception of data frames. Numeric simulations are conducted. The analysis is based on scenarios that show the existence of significant Doppler effect. More specifically, we show that Doppler effect, under narrow half-power bandwidth, is significant with respect to the half-power bandwidth in the ULF band, for long distance communications. Furthermore, we show that Doppler effect patterns are not necessarily linear.

Keywords Acoustic waves · Airplane underwater locator beacons · Communicating autonomous underwater vehicles · Doppler effect · Half-power bandwidth · Subsurface activity sensors · Surveillance networks · Underwater communications · Underwater acoustic vehicles · Unmanned undersea vehicles

1 Introduction

We are interested to investigate the impact that mobility has on communication among the nodes of a networked system. In particular, we take into account the Doppler effect in underwater acoustic communications. Consider the potential applications of underwater communications in order to form a monitoring and surveillance network [13], subsurface activity sensors [12], unmanned undersea vehicles [3] and airplane underwater locator beacons [18]. It is well-known that the mobility of a source or an observer has an influence on the waves that impacts communications. This is known as Doppler effect. Doppler effect can have a significant impact especially when compared to traditional wireless electromagnetic communications. For example, Marage and Mori show that the Doppler effect is almost 4 000 times greater in sonar than in radar [9] [pp. 9–11].

In this paper we address underwater communications using the Ultra Low Frequency (ULF) range[1], 0.3 to 3 kHz. The ULF band, as suggested by Stojanovic [11], is interesting because attenuation is lower, relative to higher frequencies. Hence, there is more potential for long range communications. For instance, Freitag et al. [6] have been able to make contact at a distance of 400 km at 900 Hz. On the other hand, the half-power bandwidth is narrow in the ULF band. As a consequence, solely extremely low rate data streams can be supported.

Given the narrow half-power bandwidth and slow propagation speed of underwater acoustic waves, one may expect a significant Doppler effect in the ULF band. The goal of this

✉ J. Garcia-Alfaro
jgalfaro@ieee.org

[1] School of Engineering, Lebanese International University, Bekaa, Lebanon

[2] School of Computer Science, Carleton University, Ottawa, ON, K1S 5B6, Canada

[3] Telecom SudParis, CNRS Samovar, UMR 5157, Evry, France

[1] Some authors also refer to this range as *Low Frequency* [5] or *Very Low Frequency* [7].

Published online: 11 April 2018

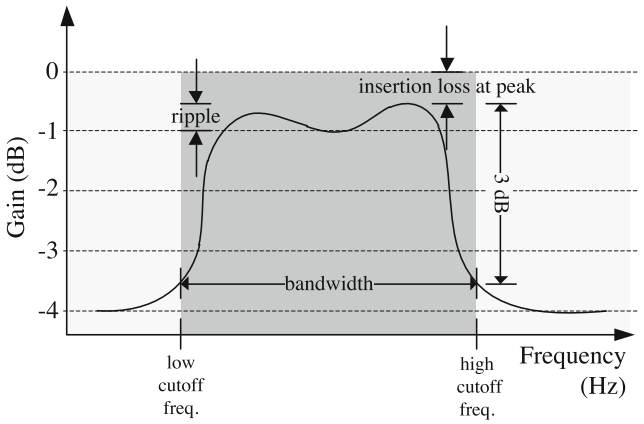

Fig. 1 Cutoff frequencies are points where the output signal level drops by three dB, with respect to the peak signal in the passband. Filter bandwidth corresponds to the difference between high cutoff and low cutoff frequencies

work is to characterize the importance of the Doppler effect in various underwater communication scenarios in the ULF band. Some questions addressed are:

- What is the maximum Doppler effect that can be expected on underwater links in the ULF band?
- What is the maximum frequency drift, and associated patterns, that can occur during the reception of a data frame?

Through a number of scenarios, and assuming either single or multiple transmitter-receiver pairs, we show that the Doppler effect is significant in the ULF band for long distances, relative to the narrow half-power bandwidth (cf. Fig. 1). We also illustrate that Doppler effect patterns are not always linear. We simulate several mobiliy scenarios, including collateral motion, transverse motion, meandering current motion, vertical and diagonal oscillation (reflection and refraction) and multipath.

The outline of the paper is as follows. Section 2 provides background on ULF underwater acoustic communications. Section 3 discusses the Doppler effect, presents our experimental scenarios and provides the results obtained. Section 4 provides the conclusion and makes suggestions for further research.

2 ULF underwater acoustic communications

Attenuation is an important impairment in underwater acoustic communication. The main causes are conversion of acoustic energy into heat as well as geometrical spreading. The magnitude of attenuation is represented in Thorp's model [15–17]. For long distance underwater communications, the ULF band is preferable because there is less attenuation at the lower end of the acoustic spectrum.

Figure 2a plots the attenuation as a function of distance for selected frequencies in the ULF band.

Realistically, for long range underwater acoustic communications, solely the use of low frequencies can be envisioned. For instance, Freitag et al. [6] have been able to achieve communication over a 400 km range at 0.9 kHz.

Another important fact is the gradient of the attenuation versus frequency. The transmission loss increases rapidly for higher frequencies. It limits the operating bandwidth. This constraint is captured by the concept of half-power bandwidth. The half-power bandwidth is commonly used to define cutoff frequencies and bandwidths of filters by

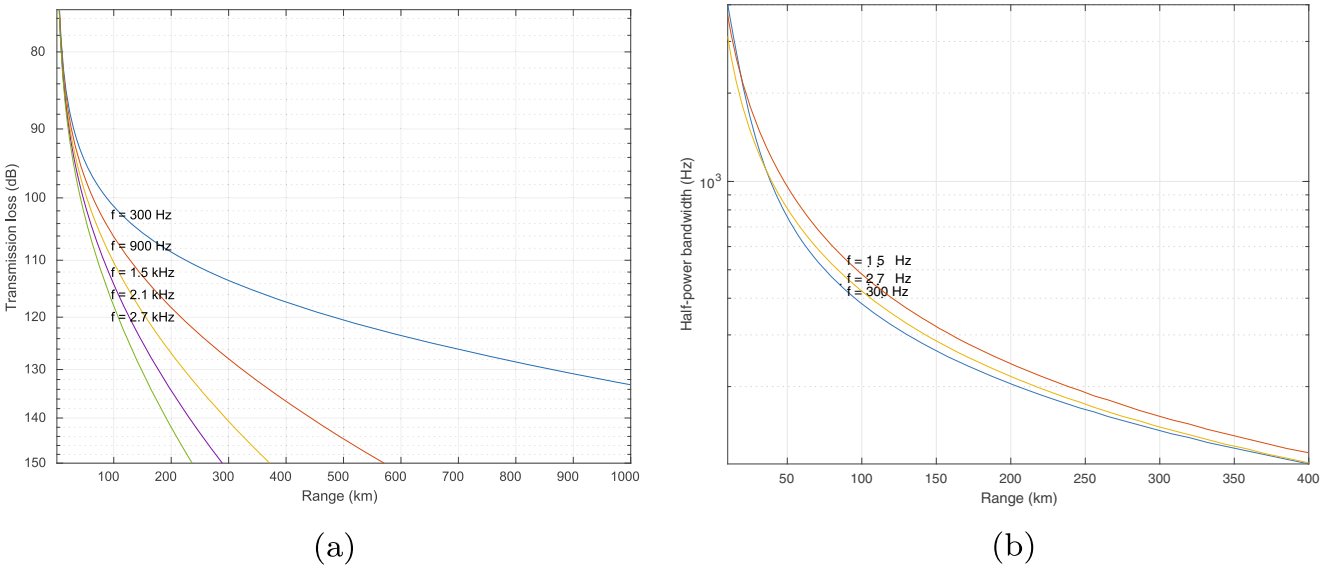

Fig. 2 In the ULF band, **a** attenuation and **b** half-power bandwidth vs range. For a range greater than 17 km, the half-power bandwidth is wider for high frequencies than for low frequencies, for the same range

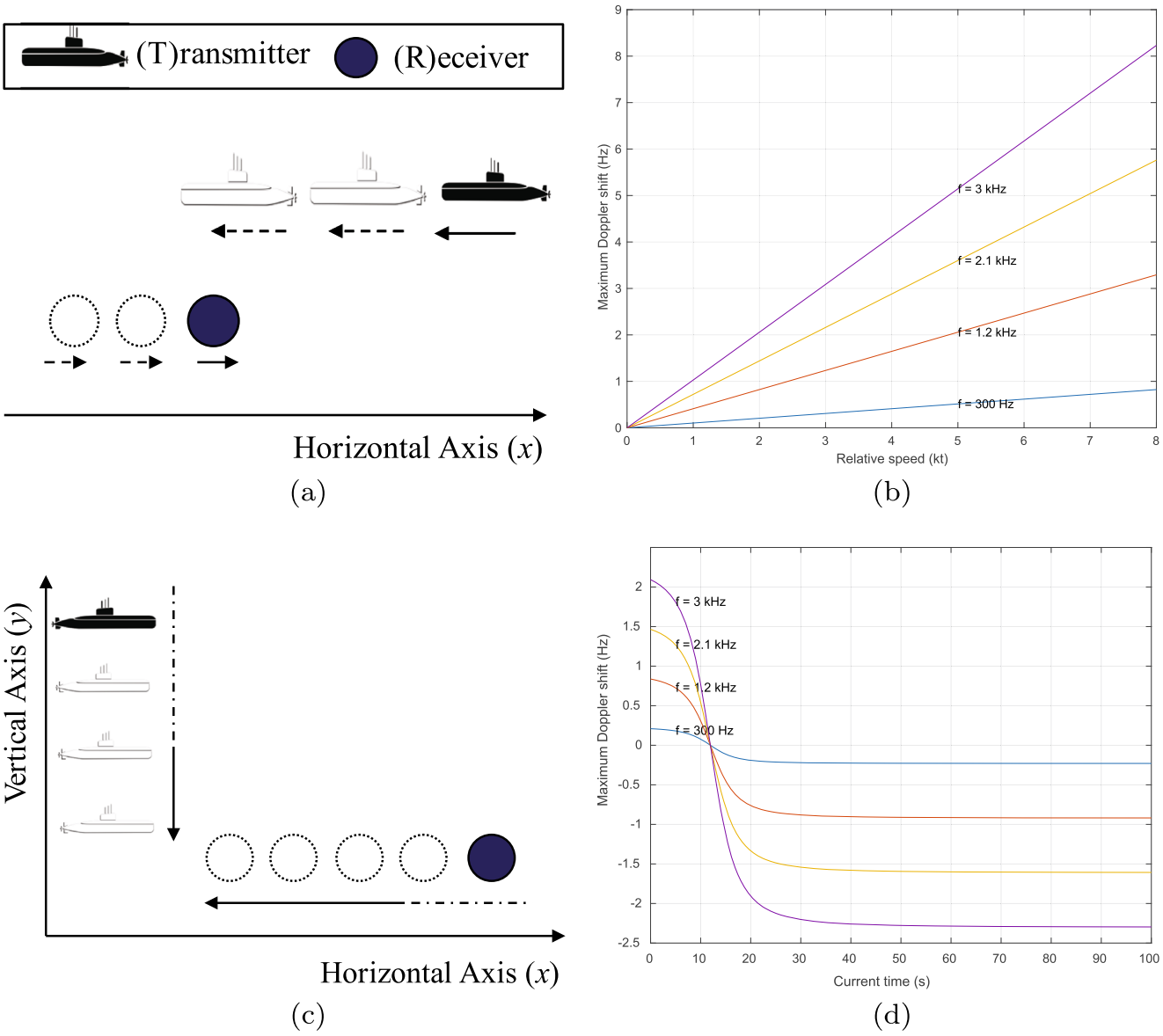

Fig. 3 Collateral and transverse motion Doppler effect scenarios. **a** Transmitter and receiver moving with collateral motion on the horizontal axis. **b** Doppler effect results w.r.t. the collateral motion scenario. **c** Transmitter and receiver moving in transverse directions. **d** Doppler effect results w.r.t. the transverse motion scenario

using frequency response curves, using 3 dB points in the frequency response of a band-pass filter [19].

Figure 2b shows the half-power bandwidth for selected ULF frequencies versus distance. Firstly, the relationship between frequency, half-power bandwidth and distance is not linear. Secondly, at very long ranges (e.g., 400 km), the half-power bandwidth is very narrow, i.e., around 0.1 kHz.

3 Experimental scenarios and results

Experiments are conducted using numeric simulations via MATLAB [10]. We assume situations in which one mobile transmitter (representing an autonomous underwater vehicle) is continuously transmitting acoustic waves at a specific frequency. At an initial distance, the waves are processed by an array of receivers (underwater sensors equipped with acoustic hydrophones). The array of receivers also moves with respect to a mobility model. For instance, the array of receivers may oscillatie according to a sinusoidal law. At each instance, one or more hydrophones of the array of receivers process a series of LOS (Line of Sight) signals from the transmitter. Our goal is to study variations of frequency shifts and estimate the detection accuracy in a series of communication scenarios. The source code of the simulations is available online at http://j.mp/UWDoppGIT.

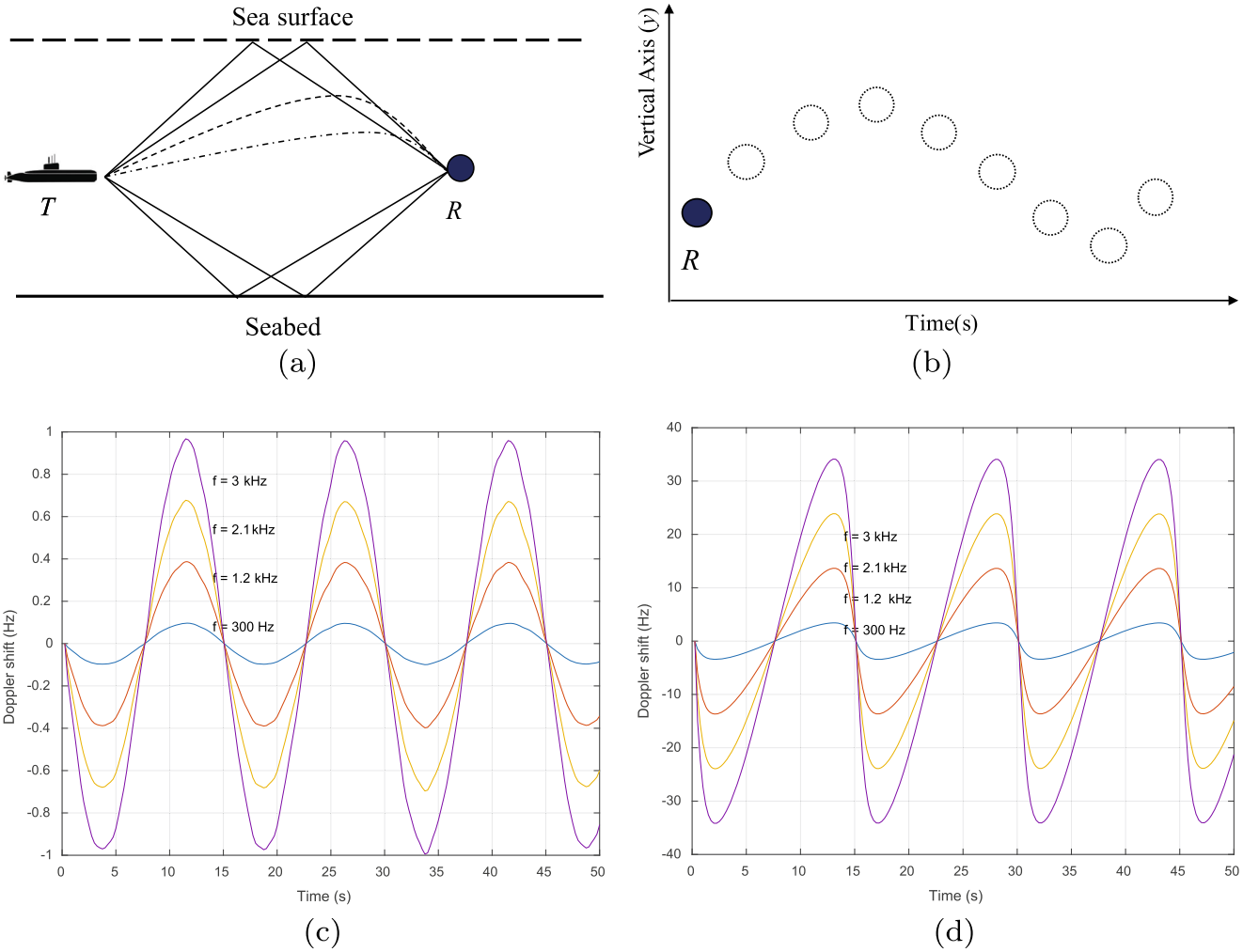

Fig. 4 **a** Communication between a stationary transmitter and a receiver. **b** The receiver oscillates vertically, according to a sinusoidal law. Straight lines represent reflected waves. Dashed lines represent refracted waves. **c, d** Doppler effect at different receiver positions for selected ULF frequencies. **c** assumes that R's motion amplitude A is 10 m. **d** assumes that R's motion amplitude A is 50 m

In all the experimental situations, we evaluate the Doppler effect from the receiver's point of view. Each shift may affect the frequency of the acoustic waves traveling to the receiver, due to the transmitter-receiver delay change during the transmission. This happens when either the transmitter or receiver are mobile. Their relative separation distance is not constant. Let v (m/s) be the relative velocity between a transmitter and a receiver. It is positive when they are getting closer and negative when moving away. Let c be the signal propagation speed (m/s). At nominal frequency f_0 Hz, the variation of frequency due to the Doppler effect is [8]:

$$\delta f = f_0 \frac{v}{c} \text{ Hz} \tag{1}$$

3.1 Collateral and transverse motion scenarios

Figure 3a provides our initial scenario. Transmitter and receiver move with collateral motion on the horizontal axis. Figure 3b depicts the maximum Doppler effect for selected frequencies in the ULF range, assuming that the relative speed varies from zero to eight knots, along the same axis. Knots are a speed measurement that is nautical miles per hour (approximately, one knot corresponds to 1.15 mile per hour, i.e., 1.8 kilometer per hour or 0.51 meter per second). The assumed range (zero to eight knots) is consistent with the values reported by Robert et al. [3] about the speed range of AUVs. The results in Fig. 3b show that the Doppler effect turns out to be linear with respect to the relative speed, if we assume that both transmitter and receiver are moving along the same axis.

Figure 3c makes the assumption that the transmitter and receiver move in transverse directions (i.e., transmitter and receiver move in opposite directions with respect to a reference axis) with constant speeds. After sligthly more than ten seconds, both of them arrive at the same point, where the Doppler shift becomes null (cf. Fig. 3d). Then,

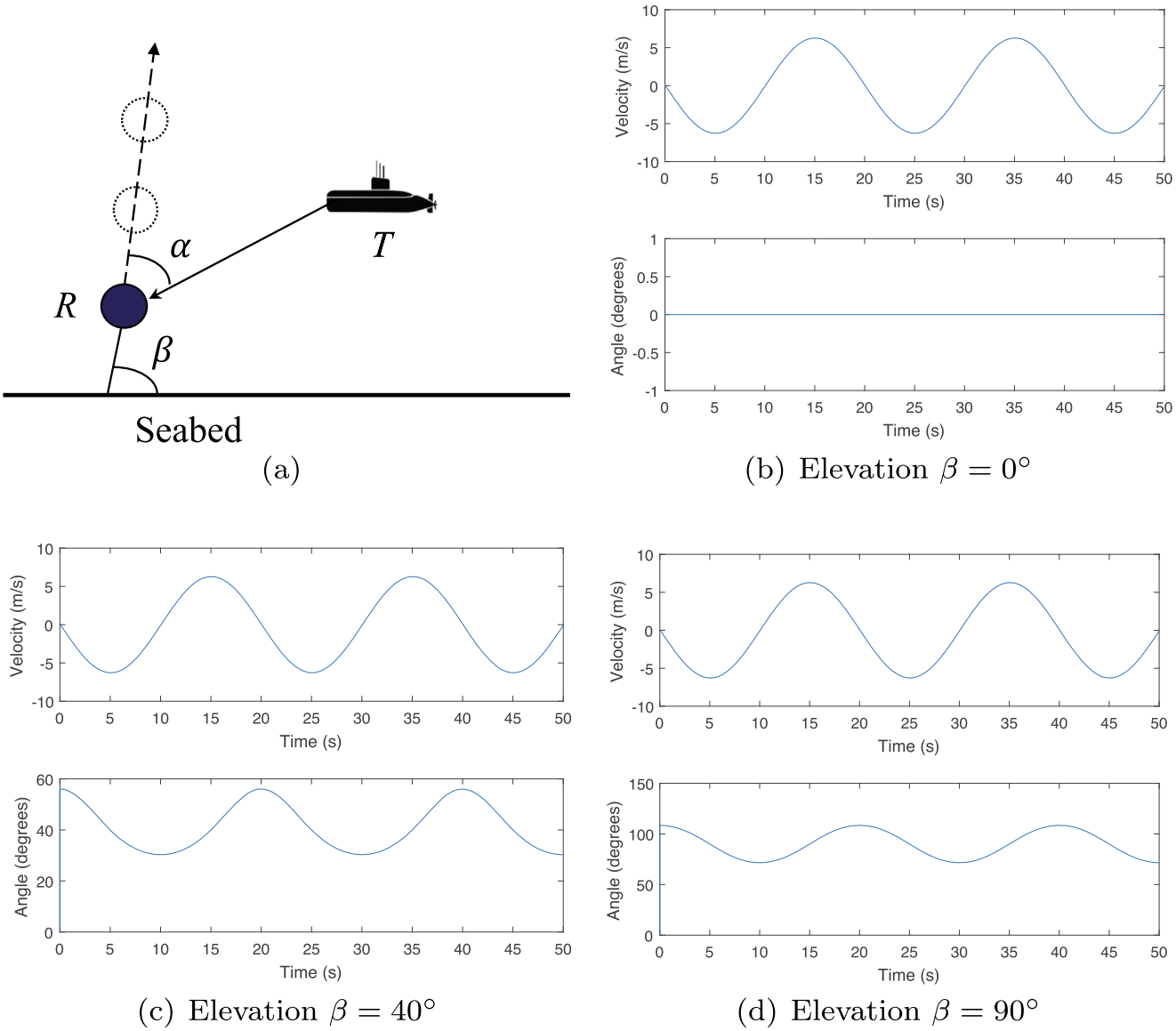

Fig. 5 **a** Underwater communication between a stationary transmitter, and a mobile receiver subject to a diagonal oscillation motion. **b** Mobility characteristics of the receiver, assuming a frequency of 1.5 kHz and elevation β equal to 0, 40 and 90°

they move away from each other, causing an increase in the Doppler effect.

3.2 Vertical oscillation (reflection and refraction) scenario

Figure 4a depicts a stationary underwater transmitter (T) conducting acoustic communication with an underwater receiver (R). As shown in Fig. 4b, R oscillates vertically, according to a sinusoidal law (such that $y(t) = A \sin\left(\frac{t \cdot \pi}{15}\right)$, where A represents the amplitude of the motion). The corresponding shift is derived according to Eq. 1 (c is 1500 m/s). The distance between the transmitter-receiver pair is derived using Euclidean distance. Distance changes are used to compute the relative velocity between T and R. The data is produced at one sample per second. The scenario assumes reflection (straight lines) and refraction (dashed lines) of waves. Reflection and refraction of waves is derived using BELLHOP [14].

Figures 4c, d plot the Doppler effect for times from $t = 0$ to $t = 50$ seconds. Figure 4c, the amplitude A of R is 10 m. The figure shows a slight frequency shift, that is one Hz at its maximum. In Fig. 4(d), the amplitude A of R is 50 m. The Doppler effect becomes noticeable, as it peaks at 3 kHz.

3.3 Diagonal oscillation scenario

Figure 5a extends the scenario in Section 3.2. The transmitter is stationary. The receiver is moving with velocity

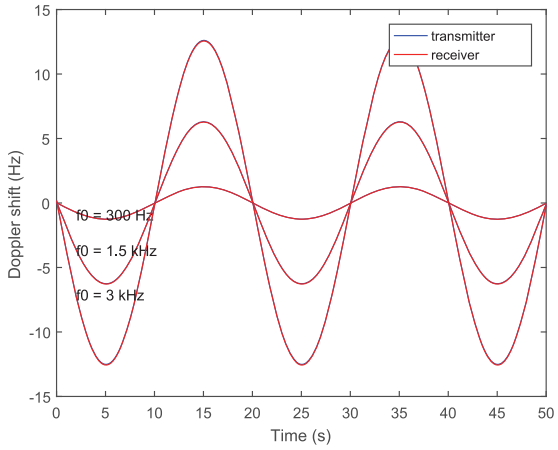

(a) Elevation $\beta = 0°$

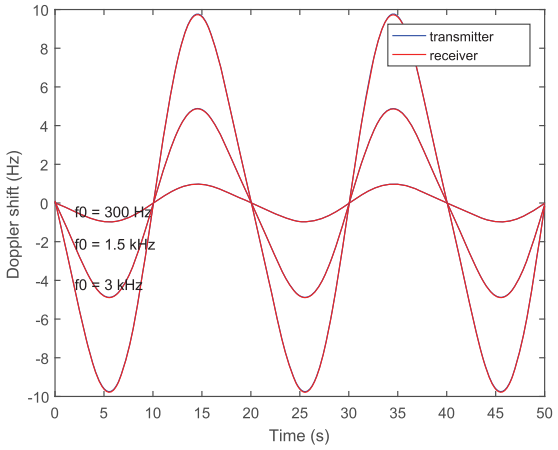

(b) Elevation $\beta = 40°$

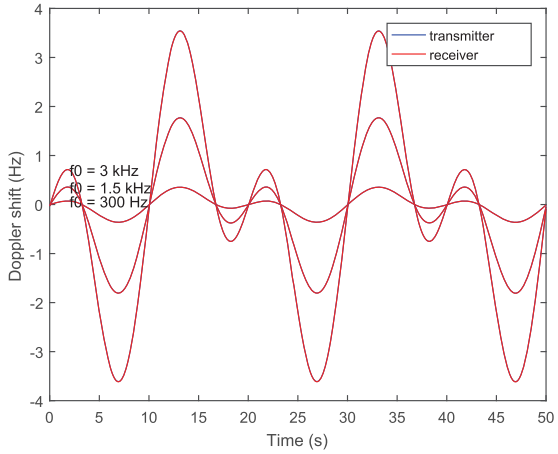

(c) Elevation $\beta = 80°$

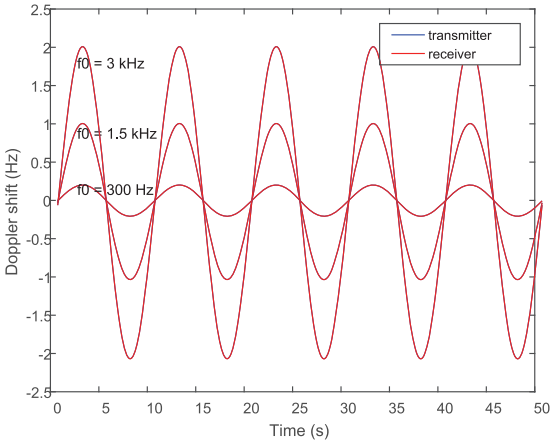

(d) Elevation $\beta = 90°$

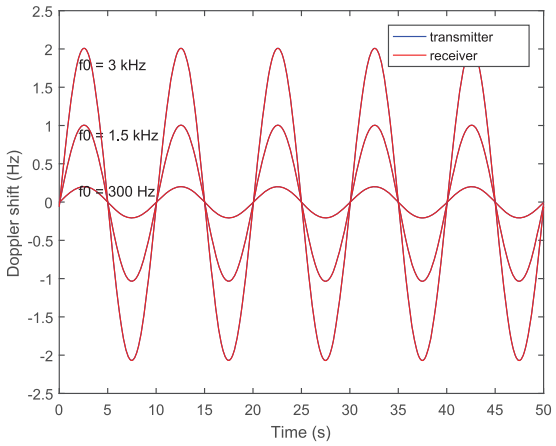

(e) Normal velocity

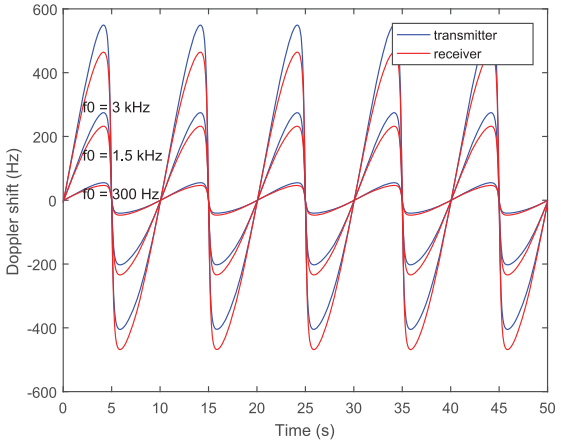

(f) 40x velocity increase

Fig. 6 **a-d** Doppler effect variation assuming a frequency of 1.5 kHz and elevation β equal to 0, 40, 80 and 90°. **e, f** Doppler shift variation from normal velocity (**e**) to 40x velocity increase (**f**)

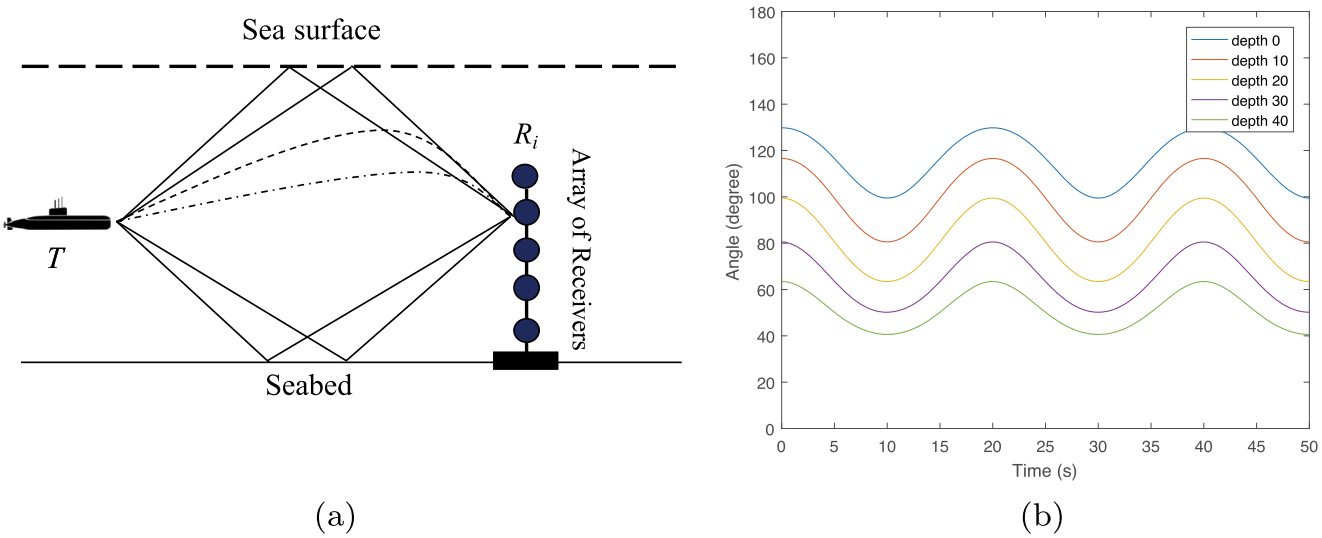

Fig. 7 **a** Underwater communication between a mobile transmitter and a stationary receiver. **b** Mobility pattern of the transmitter, drifting with two degrees of freedom, as in the meandaring model by Caruso et al. [1, 4]

w along a line with constant elevation β ($0° \leq \beta \leq 180°$). Variable α is the angle between this line and transmitter-receiver line. The receiver is assumed to follow a sinusoidal motion with frequency f_m at 0.1 Hz and amplitude of 10 m. The horizontal and vertical position x, y of the receiver is computed as follows:

$$x = \cos\beta \cdot A \cdot \cos(\pi t \cdot f_m)$$
$$y = \sin\beta \cdot A \cdot \cos(\pi t \cdot f_m)$$

The frequency f_r sensed at the receiver is computed using the following equation:

$$f_r = \left(1 + \frac{w \cdot \cos\alpha}{c}\right) \cdot f_s \tag{2}$$

where f_s is the frequency of the acoustic waves emitted by the transmitter, c is the signal propagation speed (assumed to be 1500 m/s), and w is the velocity of the receiver. The value of w is obtained by computing $\frac{\delta d}{\delta t}$, where δd is the change of distance during an interval of time t. The Doppler

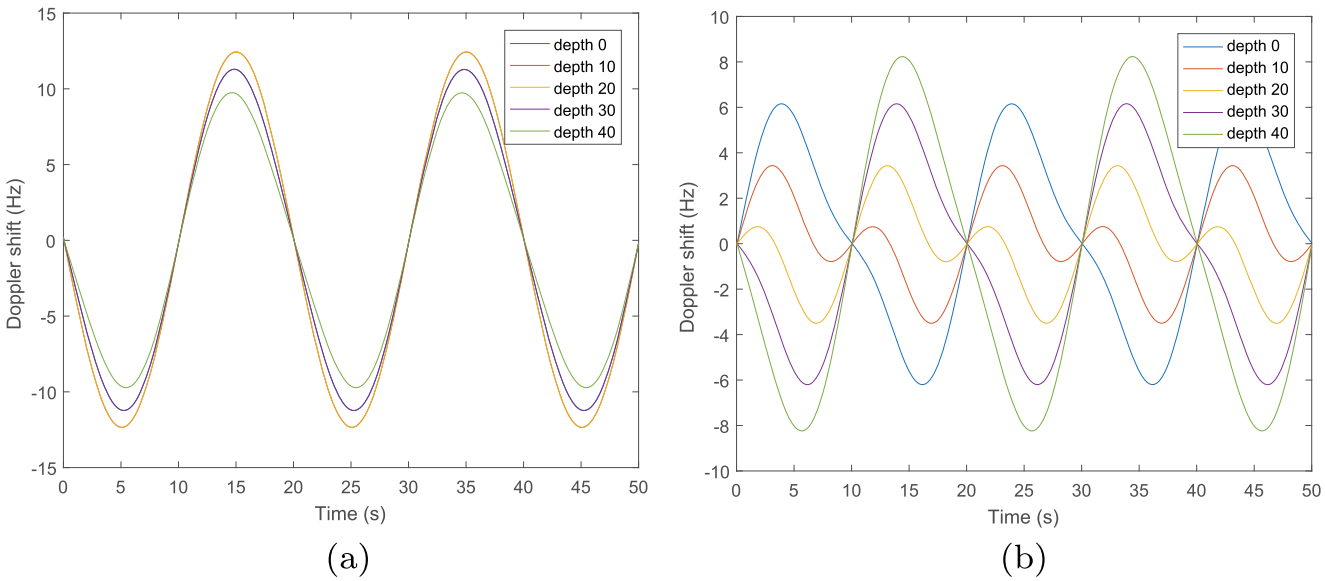

Fig. 8 Doppler effect affecting the meandaring current motion scenario. **a** Doppler effect, when the elevation β is 0°. **a** Doppler effect, when the elevation β is 90°.

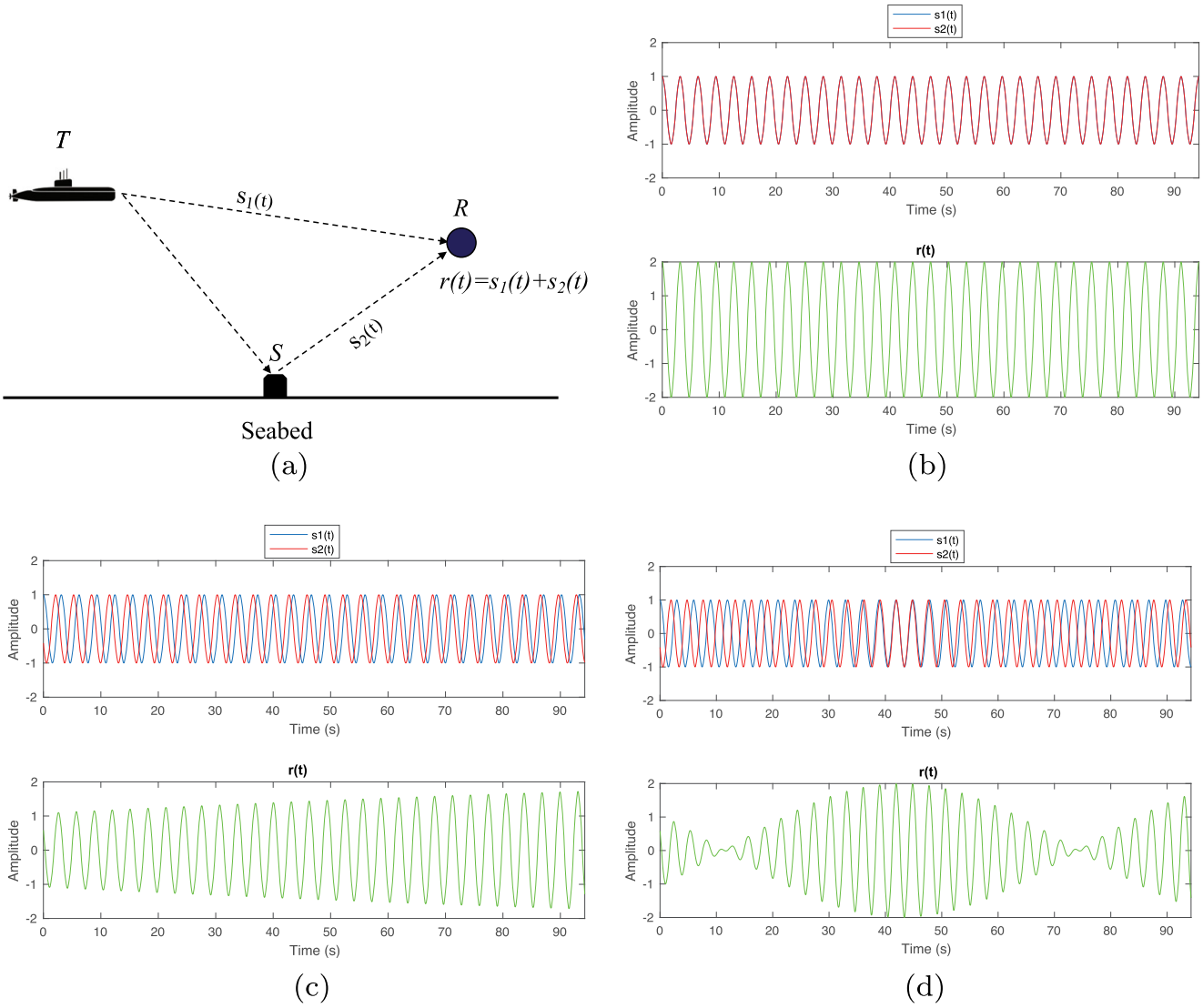

Fig. 9 **a** Assumed scenario for the multipath fading signal experiments. **b** Stationary case. No fading takes place. **c** Transmitter and reflective object move and slow fading occurs. **d** Transmitter and reflective object move, and fast fading occurs. Videocaptures with additional experiments are available at http://j.mp/UWDoppMP01

shift results are plotted in Fig. 6. The plots show the variation of the Doppler effect assuming the elevation β of 0, 40, 80 and 90°. In addition, Fig. 6e and f show the variation of the Doppler effect assuming an increase of velocity up to 40 times.

3.4 Meandaring current motion scenario w.r.t. array of receivers

Figure 7 assumes a transmitter in motion, that drifts with a two-degree of freedom motion, according to the model in [1, 4]. It transmits acoustic waves to an array R_i of receivers. Initially, the transmitter is positioned at a depth of 15 m. Five receivers are placed 30 m away from the transmitter, at depths zero, 10, 20, 30, and 40 m. The array of receivers is stationary. The following cases are considered:

1. The transmitter is moving along a line parallel to the horizontal axis, where $x = 10\cos(0.1\pi t)$ m. Depth is constant at 15 m.
2. The transmitter is moving along a line parallel to the vertical axis, where depth $d = 15 + 10\cos(0.1\pi t)$ m and $x = 0$ m.

Let v be the velocity of the transmitter. The following equation is used to compute the Doppler effect:

$$\delta f = \frac{c}{(c - v) \cdot \cos\alpha} \tag{3}$$

where α is the angle between the line along which the transmitter is moving w.r.t. the receiver line. Figure 8 shows the results. When the elevation β changes from 0 to 90°, the relative distance to the receivers gets greater than the

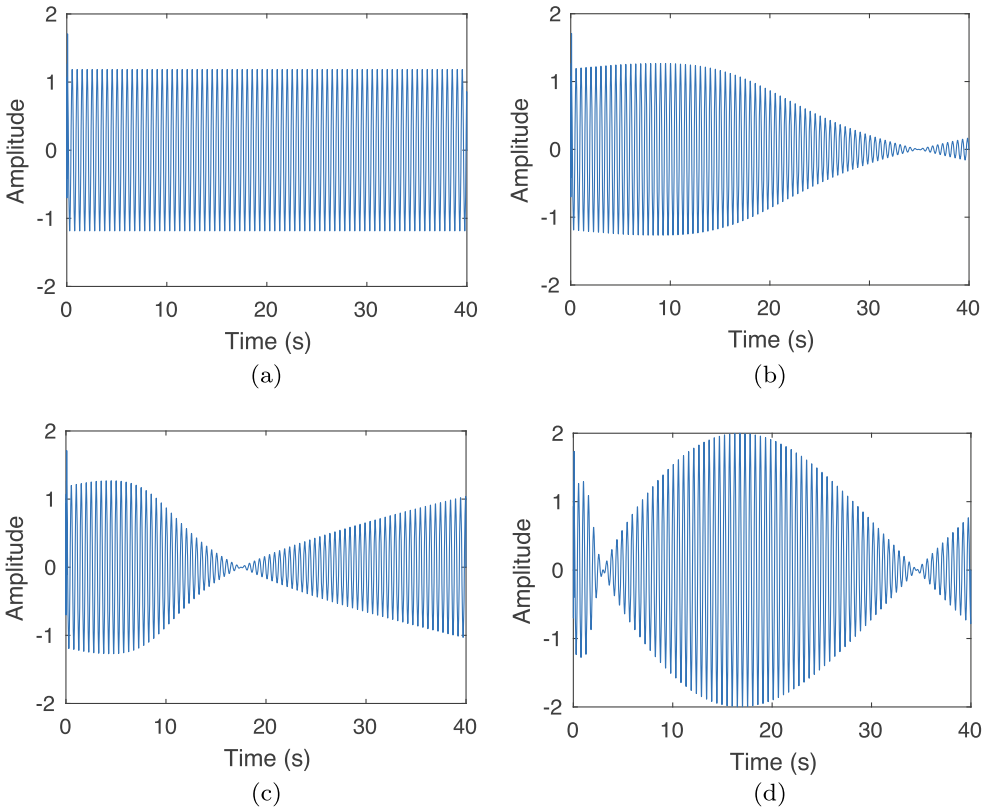

Fig. 10 Multipath fading experiments w.r.t. velocity changes (cf. videocaptures at http://j.mp/UWDoppMP02). **a** Both T and S are stationary, i.e., no fading occurs. **b** T and S move at 5 m/s and slow fading appears. **c** T and S move at 10 m/s and fast fading starts. **d** T and S move at 60 m/s and fast fading continues

amplitude of the meandering motion of the transmitter, i.e., each receiver is either above or below the transmitter. If the transmitter moves up, then it gets closer to the receiver placed at the higher depth. As the transmitter moves away from the receivers placed at the bottom of the array, the Doppler effect get its peak. When the relative motion of the transmitter is along the horizontal axis, all the receivers experience similar delays. At depths 10 to 20 m, the Doppler effect is the same as at depths 0 and 30 m — since the transmitter is moving in the middle at depth 15 m.

3.5 Multipath experiments

We investigate a fading phenomenon in ULF underwater communications due to Doppler effect and multipath propagation. Fading refers to the distortion that a modulated wave is subject to because of the propagation characteristics of the medium. We assume that multipath is due to reflection of waves on environmental boundaries, i.e., seabed and sea surface, and reflective objects, such as UAVs, underwater cliffs, vessels and icebergs. When we have multipath involving different reflective objects, an observer may get different arrivals with different Doppler effects.

A representation of this effect is depicted in Fig. 9a. There is a transmitter T, a receiver R, and a reflective object S. The signal transmitted from T travels through two different paths.

- $s_1(t)$ is the signal received by R on the direct path from T.
- $s_2(t)$ is the signal received by R through the reflective path bouncing on S. $r(t)$ is the sum of the two signals.

Figure 9b-d show three Doppler shift experimental results based on the scenario depicted in Fig. 9a. For each path, represented by $s_1(t)$ and $s_2(t)$, there is a different timing and Doppler shift profile. We assume a unit signal amplitude. The carrier signal frequency is 300 Hz.

In Fig. 9b, T, R and S are stationary. There are only phase differences in this initial case. There is no Doppler effect. In Fig. 9c, T and S move at a constant velocity, in parallel to the horizontal axis. For R, the relative radial velocity[2] of S is slower than the one of T. Given the radial velocity imbalance, there are phase and Doppler shift differences. As a result of the signal $r(t)$, we have slow fading. In Fig. 9d, T and S move at a higher velocity. In this case, we observe a larger Doppler effect difference. The resulting signal $r(t)$ is subject to fast fading.

Figure 10a-d depict a second round of Doppler effect experiments based on the scenario in Fig. 10a and velocity changes in both T and S with respect to R. The first experiment, plotted in Fig. 10a, shows the results of the stationary case (T and S are both stationary). We assume

[2]The radial velocity of T and S, with respect to R, is the rate of distance change between T and R, and S and R, respectively [2].

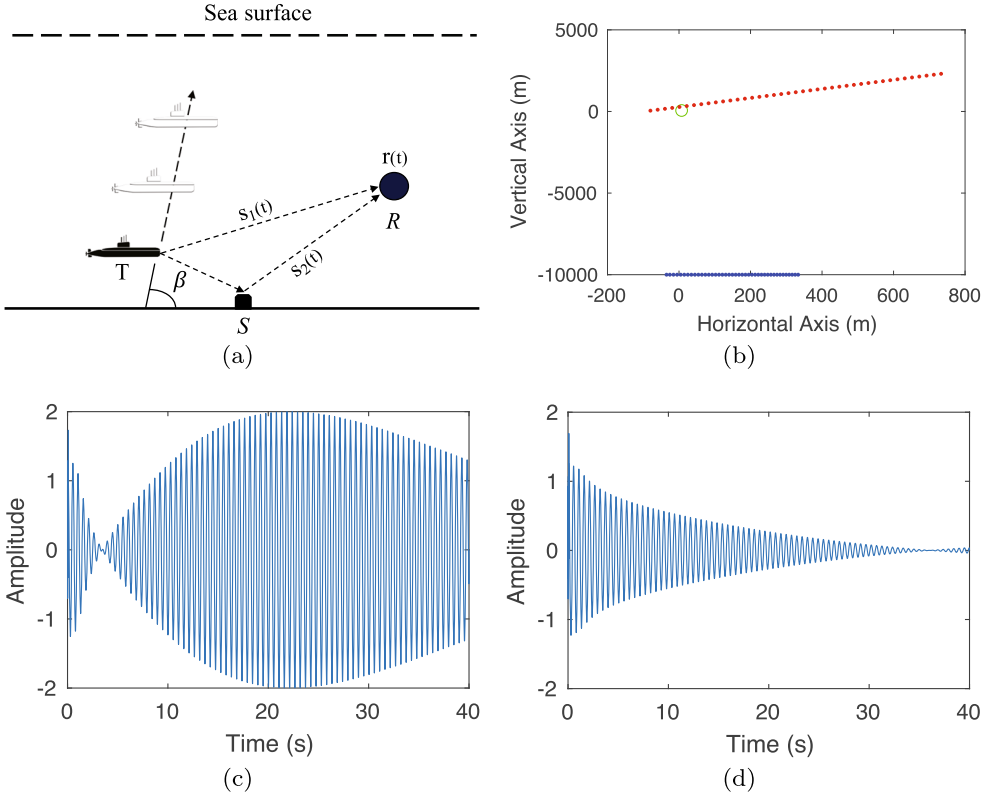

Fig. 11 Multipath fading experiments w.r.t. velocity and elevation changes of T and S. **a, b** Assumed model and patterns. **c** T and S move at 90 m/s with an elevation β of 20°. **d** T and S move at 90 m/s with an elevation β of 60°

that the conditions are such there is two degree phase difference between $s_1(t)$ and $s_2(t)$. Figure 10b shows the results of the second experiment. T and S move at a constant velocity of 5 m/s, in parallel to the horizontal axis. This movement causes a Doppler coefficient (ratio v/c in Eq. 1) of 0.013. The 300 Hz signal shifts in the $296.1 - 303.9$ Hz range. Figure 10c shows the following experiment. T and S move at constant speed of 10 m/s along the horizontal axis. This movement causes a increase in the Doppler coefficient of 0.034. The 300 Hz signal shifts in the $290 - 310$ Hz range. The direct and reflected path length difference causes that the two signals $s_1(t)$ and $s_2(t)$ to get out of phase. The signal $r(t)$ sensed by R is subject to fast fading. As the speed increases (e.g., Fig. 10d), the fading at R augments as well.

Figure 11 shows additional experiments in which T changes its elevation angle β along the vertical axis. Figure 11a, b depict the assumed patterns. Figure 11c shows that as the elevation of T increases, and it gets closer to the sea surface, fading reduces considerably. Results in Fig. 11d show that the effect of fading is at the lower amplitude areas. They decrease as the velocity and elevation of T increases. Frequency also increases proportionally to the velocity of T and the carrier frequency. Additional results are available online at http://j.mp/UWDoppMP02. Videocaptures show live evaluation of the parameters depicted in Figs. 10 and 11.

4 Conclusion

We have addressed acoustic communications between AUVs, USs and remote operators. We studied scenarios comprising one transmitter and one or several receivers. Due to the mobility of nodes, the Doppler effect changes the communication frequency. We focused on the ULF band, i.e., the frequency range 0.3 to 3 kHz. Numeric simulations confirm the importance of the Doppler effect. We have a maximum Doppler effect of 10 Hz in the scenarios we studied. It is negligible for short and medium ranges. It is, however, significant with respect to the half-power bandwidth for long distance communications (400 km). It corresponds to 10% of the theoretical half-power bandwidth. Since attenuation also depends on frequency [15–17], a positive Doppler effect increases the frequency and augments the attenuation, and vice-versa.

The source code of the simulations (collateral motions, transverse motions, vertical oscillation, meandering current motion, diagonal oscillation and multipath) is available online at http://j.mp/UWDoppGIT. Videocaptures of some of the simulated scenarios are also available online at http://j.mp/UWDoppMP01 and http://j.mp/UWDoppMP02 and http://j.mp/UWDoppMP02. From the simulated scenarios, we conclude the following. In the case of collateral motions,

in the zero to eight knot range, we have constant relative velocity. The Doppler effect is constant zero to 8 Hz. For transverse motions, the Doppler effect is non-linear variable in time. With a transmitter with meandering current motion, and a receiver that is subject to vertical oscillation, the Doppler effect is non-linear variable in time, up to 35 Hz. Regarding a transmitter with diagonal oscillation, the Doppler shift is non-linear variable in time (up to 15 Hz), decreasing with elevation. Finally, when multiple receivers are in motion, they observe different shifts.

The study of the impact of the Doppler effect in underwater communication is full of open problems. For further research, it would be interesting to look at additional frequency ranges, more general mobility patterns, as well as other effects like reflection due to surface displacements and refraction caused by the non-uniformity of the underwater medium.

Acknowledgements This work was partially supported by the Natural Sciences and Engineering Research Council of Canada (NSERC). We would also like to thank Dr. Stéphane Blouin for fruitful discussions on the topic of this paper.

References

1. Barbeau M, Blouin S, Cervera G, Garcia-Alfaro J, Hasannezhad B, Kranakis E (2015) Simulation of underwater communications with a colored noise approximation and mobility. In: 28th IEEE canadian conference on electrical and computer engineering (CCECE 2015), Halifax, NS, 2015, pp 1532–1537
2. Blouin S, Mahboubi H, Aghdam AG (2017) Long-range passive doppler-only target tracking by single-hydrophone underwater sensors with mobility. In: Migliardi M, Merlo A, Al-HajBaddar S (eds) Adaptive Mobile Computing, chap 4, pp 65–82
3. Button RW, Kamp J, Curtin TB, Dryden J (2009) A survey of missions for unmanned undersea vehicles https://www.rand.org/content/dam/rand/pubs/monographs/2009/RAND_MG808.pdf
4. Caruso A, Paparella F, Vieira LFM, Erol M, Gerla M (2008) The meandering current mobility model and its impact on underwater mobile sensor networks. In: 27th conference on computer communications (INFOCOM 2008), pp 221–225
5. Decarpigny J, Hamonic B, Wilson O (1991) The design of low frequency underwater acoustic projectors: present status and future trends. IEEE J Ocean Eng 16(1):107–122
6. Freitag L, Partan J, Koski P, Singh S (2015) Long range acoustic communications and navigation in the arctic. In: OCEANS 2015 - MTS/IEEE Washington, pp 1–5
7. Hixson E (2009) A low-frequency underwater sound source for seismic exploration. J Acoust Soc Am 126(4):2234–2234
8. Lurton X (2002) An introduction to underwater acoustics: principles and applications. Springer, Berlin
9. Marage JP, Mori Y (2010) Sonar and underwater acoustics. Wiley, New York
10. The Mathworks Inc. Natick (2015) MATLAB version 8.5.0.197 613 (R2015a)
11. Nordrum A (2017) NATO Unveils JANUS, First Standardized Acoustic Protocol for Undersea Systems http://spectrum.ieee.org/tech-talk/telecom/wireless/nato-develops-first-standardized-acoustic-signal-for-underwater-communications
12. Otnes R, Asterjadhi A, Casari P, Goetz M, Husøy T, Nissen I, Rimstad K, Van Walree P, Zorzi M (2012) Underwater acoustic networking techniques. Springer, Berlin
13. Otnes R, Voldhaug JE, Haavik S (2008) On communication requirements in underwater surveillance networks. In: OCEANS 2008-MTS/IEEE Kobe techno-ocean, pp 1–7
14. Porter MB (2011) The BELLHOP manual and user's guide http://oalib.hlsresearch.com/Rays/index.html
15. Thorp W (1965) Deep ocean sound attenuation in the sub and low kilocycle per second region. J Acoust Soc Am 38(4):648–654
16. Thorp W (1967) Analytic description of the low frequency attenuation coefficient. J Acoust Soc Am 42(1):270
17. Thorp W, Browning D (1973) Attenuation of low frequency sound in the ocean. J Sound Vib 26(1):576–578
18. Wikipedia (2018) Underwater locator beacon https://en.wikipedia.org/wiki/Underwater_locator_beacon
19. Wu B (2015) A correction of the half-power bandwidth method for estimating damping. Arch Appl Mech 85(2):315–320